


RESEARCH ARTICLE

Open Access



LOVE ON WINGS, a Dof family protein regulates floral vasculature in *Vigna radiata*

Wuxiu Guo¹, Xue Zhang¹, Qincheng Peng¹, Da Luo¹, Keyuan Jiao^{2*} and Shihao Su^{3*} 

Abstract

Background: The interaction among plants and their pollinators has been a major factor which enriched floral traits known as pollination syndromes and promoted the diversification of flowering plants. One of the bee-pollination syndromes in Faboideae with keel blossoms is the formation of a landing platform by wing and keel petals. However, the molecular mechanisms of elaborating a keel blossom remain unclear.

Results: By performing large scale mutagenesis, we isolated and characterized a mutant in *Vigna radiata*, *love on wings* (*low*), which shows developmental defects in petal asymmetry and vasculature, leading to a failure in landing platform formation. We cloned the locus through map-based cloning together with RNA-sequencing (RNA-seq) analysis. We found that *LOW* encoded a nucleus-localized Dof-like protein and was expressed in the flower provascular and vascular tissues. A single copy of *LOW* was detected in legumes, in contrast with other taxa where there seems to be at least 2 copies. Thirty one Dof proteins have been identified from the *V. radiata*'s genome, which can be further divided into four Major Cluster of Orthologous Groups (MCOGs). We also showed that ectopic expression of *LOW* in Arabidopsis driven by its native promoter caused changes in petal vasculature pattern.

Conclusions: To summarize, our study isolated a legume Dof-like factor *LOW* from *V. radiata*, which affects vasculature development in this species and this change can, in turn, impact petal development and overall morphology of keel blossom.

Keywords: Keel blossom, Landing platform, Floral vasculature, Organ asymmetry, Dof-like factor, *Vigna radiata*

Background

The majority of flowering plants have different strategies in order to attract pollinators, such as alterations in floral color, size, scent, nectar as well as shape. These changes are, in turn, under selection by different pollinators, resulting in a collection of floral traits known as pollination syndromes [1]. It has been proposed that Faboideae species with keel blossoms show adaptation towards bee pollination [2–5]. Different petals on a keel blossom play different roles in terms of pollination: the dorsal petal (or vexillum or standard or flag) acts as a billboard to attract pollinators; the ventral petals (or keel or carina) provide a space which protects the sporophyll column; and the lateral petals (or wing or alae) together

with the ventral petals form a wing-keel complex, serving as a landing platform for the insects [4, 5]. Although we already know that *CYCLOIDEA*-like (*CYC*-like) genes are involved in the differentiation of petals along dorsal-ventral axis, it is still unclear how the elaborate petal shape is formed and how it leads to the genesis of a landing platform [6–8].

Organ shape and vasculature are closely linked during the evolution of flowering plants [9, 10]. The analyses of mutants with abnormal shape and vasculature in assorted lateral organs have provided new insights on the relationship between them [11, 12]. During leaf organogenesis, the final leaf form temporally coordinates with the formation of major veins, whereas the pattern of the minor veins does not completely reflect the final leaf shape [9]. Further studies unveiled complex mechanisms and genetic networks in the control of vascular tissue development, coordinated by different phytohormones, several signal peptides and multiple transcription factors [13–16]. Nevertheless, most of the conclusions are

* Correspondence: jiaokeyuan198653@126.com; sushihao@itbm.nagoya-u.ac.jp

²Institute of Traditional Chinese Medicine and Natural Products, College of Pharmacy, Jinan University, Guangzhou 510632, Guangdong, China

³Institute of Transformative Bio-Molecules (WPI-ITbM), Nagoya University, Furo-cho, Chikusa-ku, Nagoya, Aichi 464-8601, Japan

Full list of author information is available at the end of the article



drawn from limited model species. Hence, the scenarios in other plants are still obscure, especially when referring to the origin of novel developmental traits, such as keel blossoms.

The *Dof* genes encode plant-specific transcription factors, which have a highly conserved DNA-binding Dof domain [17–20]. *Dof* genes are ubiquitous in angiosperms, gymnosperms and other early diverged lineages such as moss and algae. However, the number of *Dof* genes is highly variable among green plants and tends to be proportional with morphological complexity of plant species [17, 20]. Many *Dof* genes (20 out of total 36 in *Arabidopsis thaliana*) are expressed in the vascular system, suggesting their roles during the development and function of vascular tissues [21, 22]. In *Arabidopsis*, different sub-clades of *Dof2.4* and *Dof5.8* are expressed in distinct early stages of leaf vasculature: *Dof2.4* is highly expressed in the primary vein of leaf primordia, while *Dof5.8* shows high expression in both primary and secondary veins, as well as petal vasculature, stamens and carpels [23, 24]. No apparent phenotype was observed in the single mutant of *dof5.8*, but it enhanced the cotyledon vascular defects of a weak allele of *auxin response factor 5–2*, indicating that *Dof5.8* functions in an auxin-dependent regulation [25]. Another close paralog *Dof3.4*, or *DOF TF OBF BINDING PROTEIN 1*, which shows similar expression to *Dof5.8*, may act redundantly in the control of leaf vascular development [26]. *Dof5.6* or *HIGH CAMBIAL ACTIVITY2*, another sub-clade of *Dof* transcription factors, predominantly exists in the vascular tissues of assorted organs and its gain-of-function mutant shows pleiotropic morphological changes including increased cambial activity [27]. A recent study found that cytokinin promotes the expression of a group of *Dof* genes designated as *PHLOEM EARLY DOF* in the procambial tissue, including *Dof1.1*, *Dof2.4*, *Dof3.2*, *Dof5.1*, *Dof5.3* and *Dof5.6* [28]. Multiple loss-of-function *Arabidopsis* *Dof* mutants exhibit variably reduced radial growth around early protophloem-sieve element cells, causing further reduction of cell number in root vasculatures [28].

In this study, we evaluated a legume crop *Vigna radiata*, also known as mung bean, which is of great economic importance in Asia. Unlike classic Faboideae species with zygomorphic flowers, a part of *Vigna* spp. including *V. radiata*, have a left-handed asymmetrical flower with the left wing-keel complex generating a landing platform [29]. By large scale mutagenesis, we isolated and characterized a floral mutant *love on wings (low)*, whose left-wing petal attaches to the ventral petal and thus, leads to a failure in landing platform formation. We observed abnormality in the petal vasculature accompanied with changes in petal shape and asymmetry. We further cloned the *LOW* locus, which encodes

a plant specific *Dof*-like transcription factor localized to the nucleus and expressed in the flower vascular tissues. A single copy of *LOW* was detected in legumes in contrast with other taxa, and we found that ectopic expression of *LOW* in *Arabidopsis* disrupted the petal vasculature. Altogether, we infer that *LOW* plays an essential role in floral vascular development of keel blossoms.

Results

V. radiata has a left-handed keel blossom

The wild-type (WT) *V. radiata* flower exhibits a left-handed keel blossom (Additional file 1: Figure S1). The right lateral petal encloses the right ventral petal, whilst the left lateral petal is inflexed over the spur developed on left ventral petal, and together they form the landing platform on the left side of the flower (Additional file 1: Figure S1A). We observed that the honeybee alighted on the left landing platform and forced its head towards the base of the dorsal petal, where there is a narrow gap for the insect to insert its proboscis to the nectary (Additional file 1: Figure S1B–C).

Characterization of the *love on wings (low)* mutant

Using large-scale gamma ray mutagenesis, we characterized one mutant, which showed defects in the landing platform formation (Fig. 1). In the mutant, unlike the WT flower, lateral petals “hugged” ventral petals tightly, thus we named this mutant *love on wings (low)*. There were basically two different types of flowers on the *low* mutant: the mild type (51 out of 100), exhibited right lateral petal development similar to the WT, but the left lateral petal enclosed the left ventral petal, hindering the formation of the left wing-keel landing platform (Fig. 1b); the other type (49 out of 100) showed severe developmental defects, in which the petal arrangement was so defected since the ventral petal enclosed the lateral petals (Fig. 1c). The two floral morphologies ratio was approximately 1:1.

Then, we dissected the newly opened *V. radiata* flower and examined the morphologies of different floral organs. In both types of the mutant flowers, the shapes of lateral and ventral petals had changed (Fig. 1). In the WT flower, two bulged structures grew outwards the base of lateral petals; however, there were three bulged structures in the mutant’s lateral petals (Fig. 1). Both the right and left lateral petals in the mutant became more curved with more symmetrical petal shapes, compared with the WT flower (Fig. 1b–c). Moreover, in the WT flower, two ventral petals formed a keel structure, while in the mutant, a single ventral petal developed into a keel-like shape, similar to the phenotype of a pea mutant, *symmetric petals 1* [7]. We did not find any obvious morphological abnormality in other floral organs.

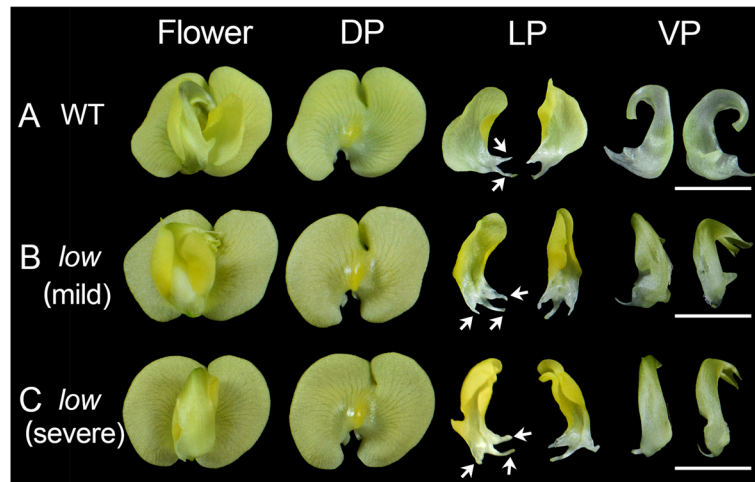


Fig. 1 Flowers of in wild-type (WT) and the *love on wings* (*low*) mutant. **a** A WT *Vigna radiata* flower. **b-c** Two types of mutant flowers. DP, dorsal petal; LP, lateral petal; VP, ventral petal. The white arrows mark the bulged structures in the base of right later petals. Bars = 10 mm

Since the plant organ shape is closely associated with organ vasculature, we then examined the petal vascular pattern in WT and mutant flowers. We dissected the 2 mm and 5 mm flower buds together with 12 mm mature flowers (Fig. 2). We found that in all the developmental stages we examined, lateral petal shape of the WT flower was more asymmetric compared with the mutant lateral petal (Fig. 2). This phenotype is consistent with changes in petal vascular pattern, especially in the main veins (Fig. 2). Petal internal asymmetry and the asymmetric vasculature

were further enhanced along with the developmental processes (Fig. 2).

As mentioned before, the single ventral petal in the mutant developed into a keel-like structure. This is also evident when we observed the ventral petals from 2 mm or 5 mm flower buds. Additional tissue of ventral petal developed in the 2 mm mutant flower (Fig. 2b). In 5 mm stage, the WT ventral petal exhibited a kidney-like shape and the spur on the left petal has not emerged yet (Fig. 2a). However, additional tissues were further grown on

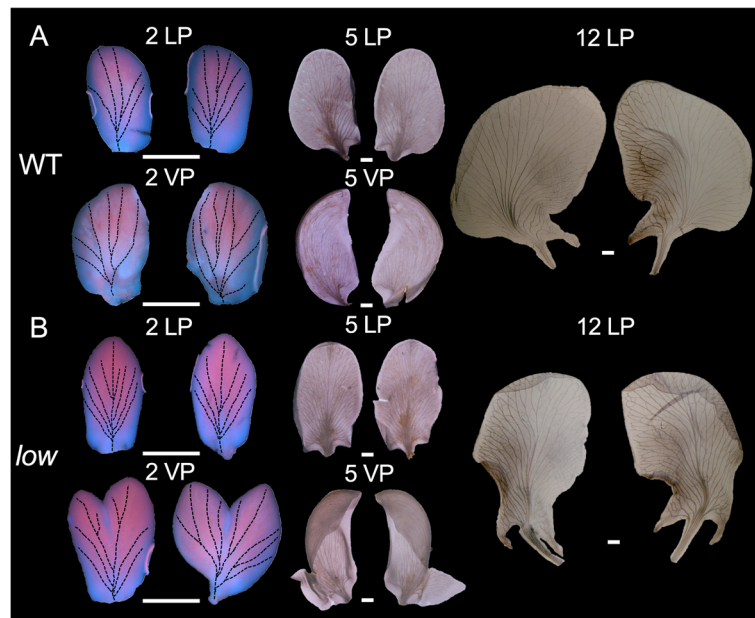


Fig. 2 Petal vasculature in wild-type (WT) and mutant. **a** Petals from WT flowers. **b** Petals from mutant flowers. 5 LP, 5 mm lateral petal; 5 VP, 5 mm ventral petal; 12 LP, 12 mm lateral petal. Bars = 2 mm

the opposite side of the mutant, forming a keel (Fig. 2b). We also noticed that vascular pattern on the ventral petal was also abnormal compared with the WT (Fig. 2). These results favor the hypothesis that changes in petal shape are linked to the defects in petal vasculature.

Cloning and phylogenetic analysis of LOW

To generate the M2 mapping population, we crossed the original mutant with another cultivar, AL127. Mutation Mapping Analysis Pipeline for Pooled RNA-seq method based on 40 individuals with mutant phenotype suggested that a large region on chromosome 7 would be the possible site where the *LOW* is located (Fig. 3a). *LOW* locus was further mapped and located between two markers, M9 and M10 (Fig. 3b). There are 54 putative genes between them and we found one candidate gene (*Vr07g10060/LOC106767037*) significantly down regulated in the mutant (Fig. 3b). *Vr07g10060/LOC106767037* encodes a Dof-like transcription factor, and we detected that in the *low* mutant, there was a 2 base-pairs

substitution followed by 11 base-pairs deletion in the Dof domain of *Vr07g10060/LOC106767037*, leading to a frame-shift and precocious termination of transcription (Fig. 3c and Additional file 2: Figure S2). Subcellular localization assay using Arabidopsis protoplasts demonstrated that green fluorescent protein fused *LOW* protein was co-localized with a nucleus marker, indicating its function possibly as a transcription factor (Additional file 3: Figure S3).

We further analyzed its orthologous proteins in different eudicots lineages (Fig. 3d). In the basal eudicot *Aquilegia coerulea*, only one copy was detected named *AcDof1*. At least one independent duplication event occurred within the diversification of rosids Salicaceae, Brassicaceae and asterids Solanaceae (Fig. 3d). However, in rosids Fabaceae, except for *Glycine max*, in which ancient whole genome duplication once occurred, only one ortholog of *LOW* exists in each legume’s genome (Fig. 3d).

To identify the DOF proteins from the mung bean genome, the consensus amino acid sequence of Dof

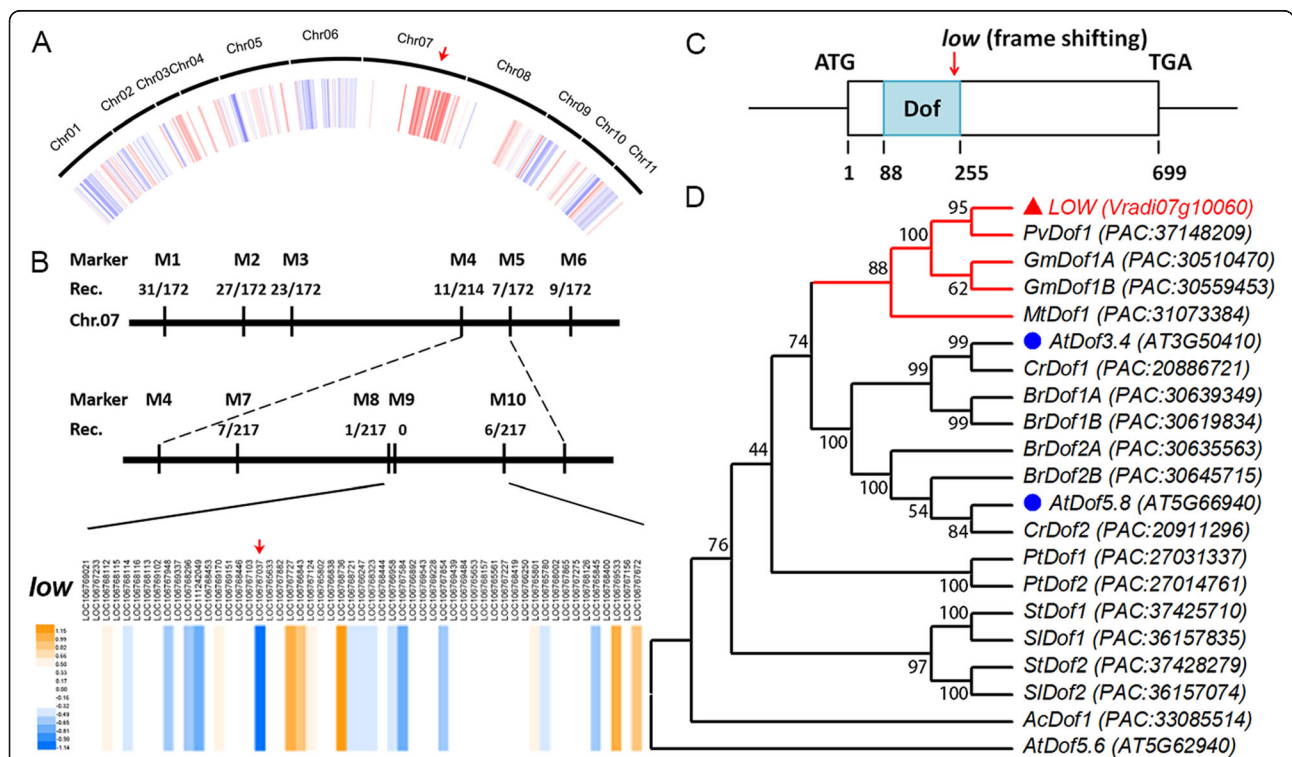
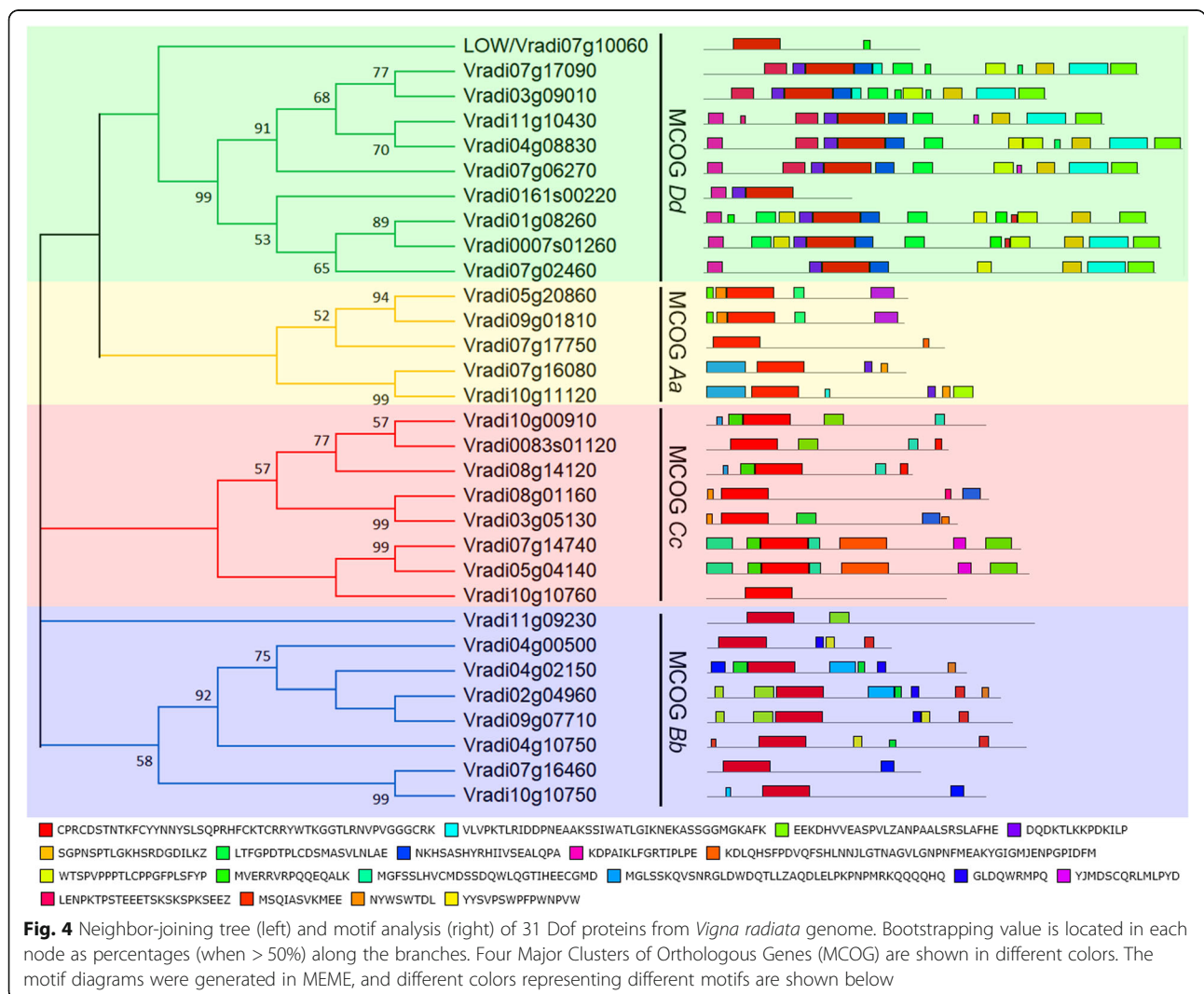


Fig. 3 Cloning and phylogeny analysis of *LOW*. **a** Association analysis based on Mutation Mapping Analysis Pipeline for Pooled RNA-seq method. The red region on chromosome 7 indicates strongest association and the red arrow marks the chromosome. **b** Physical map of the large region in Chromosome 7 of *Vigna radiata*, where *LOW* is located. Marker information (M) and recombination frequency (Rec.) are shown. In the lower lane, relative expression heat map of candidate genes between M9 and M10 is shown; the red arrow marks the *Vr07g10060/LOC106767037*. **c** The gene structure of *LOW*, nucleotide numbers, start and terminal codons are shown; the red arrow indicates the mutation. **d** Maximum-likelihood tree of *LOW*-like *Dof* genes from *Aquilegia coerulea* (*Ac*), *Arabidopsis thaliana* (*At*), *Brassica rapa* (*Br*), *Capsella rubella* (*Cr*), *Glycine max* (*Gm*), *Medicago truncatula* (*Mt*), *Populus trichocarpa* (*Pt*), *Phaseolus vulgaris* (*Pv*), *Solanum lycopersicum* (*Sl*), *Solanum tuberosum* (*St*) and *Vigna radiata* (*Vr*). 1000 times of bootstrap (value in percentage) is marked at each node and the accession number is presented in the parentheses of each sequence; the red branches highlight *LOW* and its homologs within legume species; the red triangle marks the *LOW* and blue circles indicate two paralogues from Arabidopsis. *DOF5.6* was chosen as an outgroup

domain was used to BLAST (Basic Local Alignment Search Tool) against its genome database on Legume Information System (<https://legumeinfo.org/>). Thirty one Dof proteins have been identified and all of them contain a typical Dof DNA binding domain (Additional file 4: Figure S4). To evaluate the evolutionary history among the 31 mung bean Dof proteins, we performed a phylogenetic analysis using their full length protein sequences. Phylogeny tree of these proteins indicated that Dof family have undergone multiple times of duplication (Fig. 4). Based on a previous study [30], the mung bean Dof proteins were divided into four Major Cluster of Orthologous Groups (MCOGs), which could be further divided into multiple subgroups supported by high bootstrap values and motif analysis (Fig. 4). We noticed that although LOW belongs to the MCOG Dd group, its sequence is quite different from other MCOG Dd members, indicating early divergence of this Dof protein (Fig. 4).

The spatial-temporal expression pattern of LOW

We extracted RNA from various plant tissues, and through qRT-PCR (Quantitative Reverse Transcription Polymerase Chain Reaction), found that *LOW* was highly expressed in the inflorescence with up to 2 mm flower buds (Additional file 5: Figure S5). The expression of *LOW* was rapidly decreased in later flower buds indicating that *LOW* may function in early flower developmental stages (Additional file 5: Figure S5). We further examined the spatial-temporal expression pattern of *LOW* by RNA in situ hybridization (Fig. 5a-j). The mRNA of *LOW* accumulated specifically in the central veins of flower organ primordia, including petals, stamens and carpels of early developmental stages (Fig. 5a-f). The longitudinal section of a late stage flower bud showed that *LOW* was expressed in the petals with discontinuously dot-like signals, indicating its expression in secondary petal veins (Fig. 5g). In the transverse sections of a late stage flower bud, the signals of *LOW* were accumulated in defined narrow regions within the



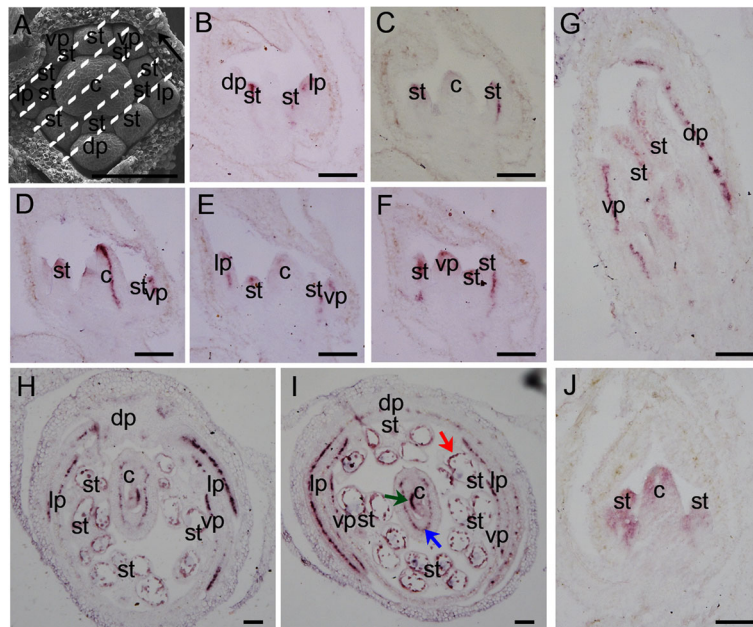


Fig. 5 The spatial-temporal expression pattern of *LOW*. **a** Flower organogenesis observed under a scanning electronic microscopy, the dot lines and the black arrow represent the places and direction, where five consecutive longitudinal sections (**b-f**) were made; dp, dorsal petal primordium; lp, lateral petal primordium; vp, ventral petal primordium; st, stamen primordium; c, carpel primordium. **b-j** The spatial-temporal expression pattern of *LOW* in wild-type (WT) *Vigna radiata* detected by RNA in-situ hybridization. **b-j** are longitudinal sections of an early flower bud; **g** shows a longitudinal section of an late flower bud; (**h-i**) show transverse sections of a late flower bud; red, green and blue arrows in (**i**) mark the tapetum, ovary and ovule, respectively. Dark brown regions in (**b-i**) represent signals detected by *LOW* antisense probe; (**J**) is a longitudinal section of an early flower bud detected by sense probe of *LOW* as a negative control. Bars = 100 μ m

petals, which were parallel with the whole flower plane (Fig. 5h-i). Moreover, the mRNA of *LOW* was detected in the anther tapetum, central ovary and ovules within a late flower bud (Fig. 5h-i).

A 2 kb DNA fragment of the *LOW* promoter region was fused to a *GUS* (β -glucuronidase) reporter gene (designated as *LOWp::GUS*) and then transformed into Arabidopsis. We detected strong *GUS* activity in the floral vasculature including pedicels, sepals, petals, filaments, styles and carpels (Additional file 6: Figure S6). The expression pattern of *LOW* in Arabidopsis system is similar to its native expression in *V. radiata*, suggesting that functional analysis of *LOW* in *A. thaliana* may help to understand its roles in *V. radiata*.

Floral phenotypes of transgenic Arabidopsis

Since the 2 kb *LOW* promoter showed specific expression in the floral vasculature of Arabidopsis, we further ectopically expressed *LOW* (designated as *pLOW::LOW*) driven by its own 2 kb promoter. Fifteen independent transgenic lines were obtained, and we carefully examined the floral morphology of each line. Petal shape in the transgenic lines was similar to the wild type plants (Fig. 6a-d). However, when comparing the petal vasculature, we found that in the WT, vascular strands usually formed four enclosed vascular loops emanating from the midvein, while in the

pLOW::LOW lines, vascular strands failed to form loops (Fig. 6a-d). These results corroborate that *LOW* functions in floral vasculature pattern.

Discussion

Co-evolution between plants and their pollinators involves changes of multiple genes among species. Although shift from one pollination syndrome to another requires complex genetic changes, it indeed occurred frequently beyond our expectations. In snapdragon, the ventral petal supported by the lateral petals is incurved at the region named hinge between the petal tube and lobe, forming a landing platform for the insects [31]. A *MIXTA*-like gene *AmMYBML1* reinforces the specialization of ventral petal hinge and thus the formation of the landing platform [31]. In another Lamiales species, *Torenia fournieri*, an ALOG family homolog TfALOG3 is essential for the development of the corolla neck, which may protect their nectar reward to pollinators [32]. In this study, we identified another class of factors from *V. radiata* involved in petal elaboration and keel blossom pattern.

Organ asymmetry has been thought to be evolved independently multiple times [33]. In terms of petal, internal asymmetry can be observed either, in dorsal and lateral petals (i.e. snapdragon and wishbone flower), or in lateral and ventral petals (i.e. many keel blossoms).



Fig. 6 Floral morphology of Col-0 (a) and three independent transgenic *Arabidopsis thaliana* lines of *pLOW::LOW* (b-d). For each plant, the upper panel exhibits an intact flower and the lower panel shows the petal vasculature. Bars = 2 mm

The first factor related to organ asymmetry was characterized in snapdragon. A *CYC*-like gene, *DICHOTOMA*, is expressed in the dorsal half of the dorsal petal primordia [33]. The *cyc dich* double mutant possesses five symmetric ventralized petals, favoring that the *CYC*-like factors couple floral dorsiventral asymmetry and petal internal asymmetry in *Antirrhinum* [33]. Unlike snapdragon, the ventral petal of a typical keel blossom is asymmetric, thus the ventralized petal should also be asymmetric. This is evident in the *Lotus japonicus* *CYC* triple mutants, where all petals become asymmetric, indicating that the floral organ internal asymmetry of a keel blossom is also related to *CYC*-like factors [34]. In pea, we previously isolated several mutants with defects in petal asymmetry, *symmetric petal 1*, *symmetric petal 5*, *elephant ear-like leaf 1* and *bigger organs*. In *syp1-1*, the petals are bilaterally symmetric and increased organs are developed among approximately 1/3 of the flowers, with abnormal primordia initiation found during early developmental stages [7]. Similar to *symmetric petal 1*, mutations in *ELEPHANT EAR-LIKE LEAF 1* and *BIGGER ORGANS* also exhibit several defects in petal asymmetry; these two proteins physically interact with each other and may act in the same genetic pathway [35]. In *symmetric petal 5* and a weaker allele of *bigger organs*, later petals in these mutants become more symmetric compared with the WT's, and genetic analysis suggests that these two factors act in an additive manner [35]. Nevertheless, unlike the *low* mutant, these mutants display other pleiotropic phenotypic defects [7, 35, 36].

In the *low* mutant, we only observed the morphological abnormalities in flower perianth, where organ asymmetry in lateral and ventral petals were abolished (Fig. 1). We also found that changes in the asymmetry of

vasculature can impact, somehow, the shape of asymmetric petals (Fig. 2), suggesting that petal vasculature development and floral dorsiventral asymmetry may interact with each other, possibly through a direct or indirect regulation of *CYC* genes or other genes involved in floral asymmetry. The transgenic *Arabidopsis* lines that bare the *LOW*'s promoter and its coding sequence, do not show any obvious changes in petal symmetry (Fig. 6). This could be due to the fact that the *LOW* construct was introduced into a heterologous system (*A. thaliana*) where endogenous *CYC* genes are likely differentially expressed and regulated, compared with what happens in *V. radiata* and other zygomorphic Fabaceae flowers.

LOW encodes a plant-specific Dof-like transcription factor. Various numbers of *Dof* genes have been found in different plant genomes with different expression patterns [17, 24]. Dof transcription factors play completely distinct roles in plant-specific processes, including light responsiveness, circadian rhythm, seed development, cell cycle regulation, phenylpropanoid metabolism, branching and vascular development [17, 18]. *LOW* was predominantly expressed in the floral vasculature (Fig. 5), which is similar but more specific comparing with the expressions of its orthologs *Dof3.4* and *Dof5.8* in *Arabidopsis* [23, 26]. According to the phylogenetic tree of *Vigna* Dof proteins, only the MCOG Dd clade that *LOW* belongs to has strong support, the other clades needs more phylogenetic analyses (Fig. 4). An interesting question is why we observed so specific floral phenotypes in the *low* mutant. Phylogenetic analysis of *LOW*'s orthologs suggested that this sub-clade of genes has undergone extensively duplication among many other plant lineages including Brassicaceae (Fig. 3d), which might explain the non-redundant function of *LOW* in

mung bean. Since the expression of *LOW* is more specific and *pLOW::LOW* transgenic *Arabidopsis* only shows abnormal vascular pattern rather than shape change, we assume that the role of *LOW* in vascular patterning is ancient, while its role in petal morphology may be an evolutionary novelty.

Dof-like transcription factors work as either transcriptional activators or repressors by binding to the sequences containing the core AAAG motif [18, 37–41]. In *A. thaliana*, a Dof-like transcription factor DOF4.2 negatively affects flavonoid biosynthesis by repressing expression of genes such as *FLAVONOL-3-HYDROXYLASE*, *DIHYDROFLAVONOL REDUCTASE* and *LEUCOANTHOCYANIDIN DIOXYGENASE*, while positively influences the accumulation of hydroxycinnamic acids by promoting the expression of genes including *PHENYLALANINE AMMONIA LYASE*, *CINNAMATE-4-HYDROXYLASE* and *4-COUMAROYL-COA LIGASE 5* [37]. In *Pinus pinaster*, the PpDof5 transcription factor may regulate the expression of glutamine synthetase (GS) genes by activating the transcription of the *GS1b*, or in contrast, by repressing the expression of *GS1a* [38]. In the moss *Physcomitrella patens*, two Dof-like transcription factors, PpDof1 and PpDof2, show transcriptional repressor activities in protoplast transient assays [40]. In the fruit banana *Musa acuminata*, a Dof transcription factor MaDof23 works as a repressor, acting antagonistically in regulating ripening-related genes associated with cell wall degradation and aroma formation [41].

Conclusions

To summarize, we have characterized a legume *Dof* gene, *LOW*, which is involved in the differentiation of keel blossom by regulating floral vasculature pattern and petal internal asymmetry of mung bean. In the future, it is of interest to study how *LOW* regulates the petal vasculature and organ asymmetry at a molecular, genetic and developmental level.

Methods

Plant materials and map-based cloning

Two cultivars of *V. radiata*, Sulu and AL127, have been purified by selfing for three generations in a greenhouse at $28 \pm 2^\circ\text{C}$ with a 16 h-light/8 h-dark photoperiod at $200 \mu\text{mol m}^{-2} \text{s}^{-1}$. *A. thaliana* Col-0 were grown at $20 \pm 2^\circ\text{C}$ with a 16 h-light/8 h-dark photoperiod at $150 \mu\text{mol m}^{-2} \text{s}^{-1}$. The seeds of Sulu, AL127 and *A. thaliana* Col-0 were obtained from the germplasm bank in our lab.

The gamma ray mutagenesis was performed as we previously described [42]. *low* mutant was isolated from the M2 population of the mutagenized cultivar Sulu background. A 576 F2 mapping population was produced by crossing *low* (from the sulu background) to AL127.

RNA-seq libraries based on the published genomic data from 40 individuals with mutant phenotype were generated using Mutation Mapping Analysis Pipeline for Pooled RNA-seq method [43, 44]. This result suggested that a large region on chromosome 7 would be the possible site where the *LOW* mutation is mapped. *Low* was further mapped with the F2 population based on the marker information that we published previously [45]. The primer sequences used in mapping are listed in the Supporting Information (Additional file 7: Table S1).

Microscopy

Inflorescences or different flower buds were fixed in FAA (3.7% formaldehyde, 50% ethanol, 5% acetic acid) fixative solution prior to clearing in 95% ethanol. Floral organs from buds in a series of developmental stages were dissected and observed under a light or fluorescence microscope. Petal vasculatures of 5 mm buds and mature flowers became visible under a light microscope after fixation and clearing, while petals from 2 mm buds were observed under the ultra violet laser. For scanning electron microscopy, fixed samples were treated and observed under the Jeol JSM 6360LV (Jeol, Tokyo, Japan) scanning electron microscope as previously reported [46]. Adobe PHOTOSHOP CS6 (Adobe, San Jose, CA, USA) was used to adjust the contrast of the images.

Phylogeny analysis, motif-based sequence analysis and subcellular localization

For phylogeny analysis of Dof-like family, protein sequences were obtained from the genomic database of *Medicago truncatula* (Mt4.0) and *Vigna radiata* (Vr1.0) in the Legume Information System (<https://legumeinfo.org/home>), or the Arabidopsis Information Resource (<https://www.arabidopsis.org/>). Amino acid sequences were aligned using CLUSTALW or MUSCLE followed by the generation of a Neighbor-joining tree with 1000 bootstrap replicates in MEGA6 [47]. Further analysis of *LOW* sub-clade Dof-like factors, nucleotide sequences from *Aquilegia coerulea*, *Arabidopsis thaliana*, *Brassica rapa*, *Capsella rubella*, *Glycine max*, *Medicago truncatula*, *Populus trichocarpa*, *Phaseolus vulgaris*, *Solanum lycopersicum*, *Solanum tuberosum* and *Vigna radiata* were obtained from the Phytozome 12 (<https://phytozome.jgi.doe.gov/pz/portal.html#>). Maximum-likelihood trees of these genes were also generated with 1000 times of bootstrap in MEGA6 [47]. Dof protein sequences were submitted to motif-based sequence analysis website (MEME; <http://meme-suite.org/tools/meme>) for motif mining under the parameters: -time 18,000, -mod zoops, -nmotifs 50, -minw 6, -maxw 50, -objfun classic, -markov_order 0.

For subcellular localization, healthy leaves from 2 to 3 week-old plants of *A. thaliana* were collected for the preparation of protoplasts. The in-frame *LOW* coding

sequence was fused with a green fluorescent protein in the C-terminal region under a constitutive expression promoter *POLYUBIQUITIN 10* and was co-transformed into the leaf mesophyll protoplasts with a nucleus marker, ARF19IV-mCherry, by PEG-induced transformation as previously used [48, 49]. The fluorescent signals were observed using a confocal laser scanning microscopy Zeiss7 DUO NLO (Zeiss, Oberkochen, Germany).

qRT-PCR and RNA in situ hybridization

Plant genomic DNA and total RNA were extracted from different tissues as described [46]. For qRT-PCR, 1 µg total RNA from different tissues was reverse transcribed using PrimeScript RT reagent Kit with gDNA Eraser (Takara, Beijing, China) following the manufacturer's instructions. The PCR assays were performed under the manual of LightCycler 480 Real-Time PCR System (Roche, Shanghai, China). Briefly, the target temperature was set to 58 °C and 45 cycles were used for amplification. All the data were normalized against the expression of constitutively expressed reference gene *VrTUB* (*Vradi05g13910*) as reported [50]. The gene expression level was calculated from three biological replicates and three technical replicates. Graphs were produced by GraphPad Prism (GraphPad Software). The primer sequences used in qRT-PCR were listed in the Supporting Information (Additional file 7: Table S1).

For RNA in situ hybridization, flowers at different stages of development were fixed and treated as previously reported [51]. DNA Fragment for producing the sense and antisense probes was cloned and ligated to pTA2 plasmid (TOYOBO, Shanghai, China). Probes were then labeled with digoxigenin-UTP (Roche, Shanghai, China). The non-radioactive in situ hybridization processes were carried out as described [52]. The primer sequences used in RNA in situ hybridization were listed in the Supporting Information (Additional file 2: Table S1).

Arabidopsis transformation and GUS staining

For GUS assay, a 2 kb DNA fragment corresponded to the 5' promoter and untranslated region of *LOW* was fused to a *GUS* gene on pCXGUS-P vector as described [53]. For functional analysis, the full-length coding sequences of *LOW* was cloned and inserted into pFGC-RCS vector driven by the native 2 kb *LOW* promoter as described [53]. The plasmids were transformed into the EHA105 *Agrobacterium tumefaciens* strains and plant transformation was performed under the instruction of floral dipping method as described [54]. The seeds of transgenic plants were selected on Murashige and Skoog (MS) culture media containing proper antibiotics. Histochemical GUS staining assay was performed as described [55]. The stained tissues were examined, dissected and photographed under a stereomicroscope.

Supplementary information

Supplementary information accompanies this paper at <https://doi.org/10.1186/s12870-019-2099-x>.

Additional file 1: Figure S1. Left keel-wing complex in *Vigna radiata* functions as a landing platform for the bee pollinators. (A) Diagram of a *V. radiata* flower, the left keel and left wing are marked in pink and blue, respectively. (B) Front view of a bee visitation. (C) Side view of a bee visitation.

Additional file 2: Figure S2. Alignment of *Vr07g10060/LOC106767037* coding sequences in wild type and mutant. Box indicates mutated region in the mutant and the blue line marks the Dof domain.

Additional file 3: Figure S3. Subcellular localization of LOW-GFP fused protein. Signals from GFP, mCherry, chloroplast and merged channels are shown; nuclear marker ARF19IV-mCherry plasmid was co-transformed with LOW-GFP construct; Bars = 10 µm.

Additional file 4: Figure S4. Dof domain sequence alignment of the 31 mung bean proteins. Identical and similar (> 80%) amino acids are highlighted in black and grey, respectively.

Additional file 5: Figure S5. Quantitative RT-PCR analysis of *LOW* in different tissues, error bars of gene expression are ±1 SD from three replicates.

Additional file 6: Figure S6. GUS-stained inflorescence and floral organs of transgenic *Arabidopsis thaliana* lines of *LOWp:GUS*. Bar = 2 mm.

Additional file 7: Table S1. Primers used in this study.

Abbreviations

BLAST: Basic Local Alignment Search Tool; CYC: CYCLOIDEA; GS: Glutamine synthetase; GUS: β-glucuronidase; LOW: LOVE ON WINGS; MCOGS: Major Cluster of Orthologous Groups; qRT-PCR: Quantitative Reverse Transcription Polymerase Chain Reaction; RNA-seq: RNA-sequencing; WT: Wild-type

Acknowledgements

We thank Miss Maria João Ferreira (University of Porto, Portugal) for her constructive suggestions during manuscript revision. We are also grateful to the anonymous reviewers for their encouraging and valuable comments.

Authors' contributions

WG, DL and SS designed the research; WG, DL, KJ, XZ, QP and SS performed the research; WG, KJ and SS analyzed the data; WG and SS wrote the paper; WG, DL and SS revised the manuscript. All authors read and approved the manuscript

Funding

This work was supported by the National Natural Science Foundation of China (Grant No. 31700186) and the Chang Hungta Science Foundation of Sun Yat-sen University. S.S. is supported by an overseas postdoctoral fellowship from Japan Society for the Promotion of Science. The funding agencies had no role in the experimental design, data collection and analysis or preparation of the manuscript.

Availability of data and materials

The datasets supporting the conclusions of this article are included within the article.

Ethics approval and consent to participate

Not applicable.

Consent for publication

Not applicable.

Competing interests

The authors declare that they have no competing interests.

Author details

¹State Key Laboratory of Biocontrol and Guangdong Key Laboratory of Plant Resources, School of Life Sciences, Sun Yat-sen University, Haizhu district, Guangzhou 510275, Guangdong, China. ²Institute of Traditional Chinese

Medicine and Natural Products, College of Pharmacy, Jinan University, Guangzhou 510632, Guangdong, China. ³Institute of Transformative Bio-Molecules (WPI-ITbM), Nagoya University, Furo-cho, Chikusa-ku, Nagoya, Aichi 464-8601, Japan.

Received: 17 June 2019 Accepted: 24 October 2019

Published online: 14 November 2019

References

- Fenster CB, Armbruster WS, Wilson P, Dudash MR, Thomson JD. Pollination syndromes and floral specialization. *Annu Rev Ecol Evol S.* 2004;35:375–403.
- Aronne G, Giovanetti M, De Micco V. Morphofunctional traits and pollination mechanisms of *Coronilla emerus* L. flowers (Fabaceae). *Sci World J.* 2012;2012:1–8.
- Toon A, Cook LG, Crisp MD. Evolutionary consequences of shifts to bird-pollination in the Australian pea-flowered legumes (Mirbelieae and Bossiaeeae). *BMC Evol Biol.* 2014;14(1):43.
- Lopez J, Rodriguez-Riano T, Ortega-Olivencia A, Devesa JA, Ruiz T. Pollination mechanisms and pollen-ovule ratios in some Genisteeae (Fabaceae) from southwestern Europe. *Plant Syst Evol.* 1999;216(1–2):23–47.
- Westerkamp C. Keel blossoms: bee flowers with adaptations against bees. *Flora.* 1997;192(2):125–32.
- Feng X, Zhao Z, Tian Z, Xu S, Luo Y, Cai Z, et al. Control of petal shape and floral zygomorphy in *Lotus japonicus*. *Proc Natl Acad Sci U S A.* 2006;103(13):4970–5.
- Wang Z, Luo Y, Li X, Wang L, Xu S, Yang J, et al. Genetic control of floral zygomorphy in pea (*Pisum sativum* L.). *Proc Natl Acad Sci U S A.* 2008; 105(30):10414–9.
- Jiao K, Li X, Guo W, Su S, Luo D. High-throughput RNA-Seq data analysis of the Single Nucleotide Polymorphisms (SNPs) and Zygomorphic Flower Development in Pea (*Pisum sativum* L.). *Int J Mol Sci.* 2017;18(12):2710.
- Dengler N, Kang J. Vascular patterning and leaf shape. *Curr Opin Plant Biol.* 2001;4(1):50–6.
- Nelson T, Dengler N. Leaf vascular pattern formation. *Plant Cell.* 1997;9(7):1121–35.
- Alonso-Peral MM. The HVE/CAND1 gene is required for the early patterning of leaf venation in *Arabidopsis*. *Development.* 2006;133(19):3755–66.
- Franks RG, Liu Z, Fischer RL. SEUSS and LEUNIG regulate cell proliferation, vascular development and organ polarity in *Arabidopsis* petals. *Planta.* 2006; 224(4):801–11.
- Ruonala R, Ko D, Helariutta Y. Genetic networks in plant vascular development. *Annu Rev Genet.* 2017;51:335–59.
- De Rybel B, Adibi M, Breda AS, Wendrich JR, Smit ME, Novak O, et al. Integration of growth and patterning during vascular tissue formation in *Arabidopsis*. *Science.* 2014;345(6197):1255215.
- Mahonen AP, Bishopp A, Higuchi M, Nieminen KM, Kinoshita K, Tormakangas K, et al. Cytokinin signaling and its inhibitor AHP6 regulate cell fate during vascular development. *Science.* 2006;311(5757):94–8.
- Galweiler L, Guan C, Muller A, Wisman E, Mendgen K, Yephremov A, et al. Regulation of polar auxin transport by AtPIN1 in *Arabidopsis* vascular tissue. *Science.* 1998;282(5397):2226–30.
- Noguero M, Atif RM, Ochatt S, Thompson RD. The role of the DNA-binding one zinc finger (DOF) transcription factor family in plants. *Plant Sci.* 2013; 209:32–45.
- Yanagisawa S. The Dof family of plant transcription factors. *Trends Plant Sci.* 2002;7(12):555–60.
- Umemura Y, Ishiduka T, Yamamoto R, Esaka M. The Dof domain, a zinc finger DNA-binding domain conserved only in higher plants, truly functions as a Cys2/Cys2 Zn finger domain. *Plant J.* 2004;37(5):741–9.
- Moreno-Risueno MA, Martinez M, Vicente-Carbajosa J, Carbonero P. The family of DOF transcription factors: from green unicellular algae to vascular plants. *Mol Gen Genomics.* 2007;277(4):379–90.
- Le Hir R, Bellini C. The plant-specific dof transcription factors family: new players involved in vascular system development and functioning in *Arabidopsis*. *Front Plant Sci.* 2013;4:164.
- Gardiner J, Sherr I, Scarpella E. Expression of DOF genes identifies early stages of vascular development in *Arabidopsis* leaves. *Int J Dev Biol.* 2010; 54(8–9):1389–96.
- Konishi M, Yanagisawa S. Sequential activation of two Dof transcription factor gene promoters during vascular development in *Arabidopsis thaliana*. *Plant Physiol Bioch.* 2007;45(8):623–9.
- Shigyo M, Tabei N, Yoneyama T, Yanagisawa S. Evolutionary processes during the formation of the plant-specific Dof transcription factor family. *Plant Cell Physiol.* 2007;48(1):179–85.
- Konishi M, Donner TJ, Scarpella E, Yanagisawa S. MONOPTEROS directly activates the auxin-inducible promoter of the Dof5.8 transcription factor gene in *Arabidopsis thaliana* leaf provascular cells. *J Exp Bot.* 2015;66(1):283–91.
- Skirycz A, Radziejowski A, Busch W, Hannah MA, Czeszejko J, Kwaśniewski M, et al. The DOF transcription factor OBP1 is involved in cell cycle regulation in *Arabidopsis thaliana*. *Plant J.* 2008;56(5):779–92.
- Guo Y, Qin G, Gu H, Qu LJ. Dof5.6/HCA2, a Dof transcription factor gene, regulates Interfascicular cambium formation and vascular tissue development in *Arabidopsis*. *Plant Cell.* 2009;21(11):3518–34.
- Miyashima S, Roszak P, Sevilem I, Toyokura K, Blob B, Heo JO, et al. Mobile PEAR transcription factors integrate positional cues to prime cambial growth. *Nature.* 2019;565(7740):490–4.
- Hedström I, Thulin M. Pollination by a hugging mechanism in *Vigna vexillata* (Leguminosae-Papilionoideae). *PI Syst Evol.* 1986;154(3/4):275–83.
- Lijavetzky D, Carbonero P, Vicente-Carbajosa J. Genome-wide comparative phylogenetic analysis of the rice and *Arabidopsis* Dof gene families. *BMC Evol Biol.* 2003;3:17.
- Perez-Rodríguez M, Jaffe FW, Butelli E, Glover BJ, Martin C. Development of three different cell types is associated with the activity of a specific MYB transcription factor in the ventral petal of *Antirrhinum majus* flowers. *Development.* 2005;132(2):359–70.
- Xiao W, Su S, Higashiyama T, Luo D. A homolog of the ALOG family controls corolla tube differentiation in *Torenia fournieri*. *Development.* 2019; 146(16):dev177410.
- Luo D, Carpenter R, Copeley L, Vincent C, Clark J, Coen E. Control of organ asymmetry in flowers of *antirrhinum*. *Cell.* 1999;99(4):367–76.
- Wang J, Wang Y, Luo D. LjCYC genes constitute floral dorsoventral asymmetry in *Lotus japonicus*. *J Integr Plant Biol.* 2010;52(11):959–70.
- Li X, Liu W, Zhuang L, Zhu Y, Wang F, Chen T, Luo D. BIGGER ORGANS and ELEPHANT EAR-LIKE LEAF1 control organ size and floral organ internal asymmetry in pea. *J Exp Bot.* 2018;70(1):179–91.
- Li X, Zhuang LL, Ambrose M, Rameau C, Hu XH, Yang J, et al. Genetic analysis of ele mutants and comparative mapping of ele1 locus in the control of organ internal asymmetry in garden pea. *J Integr Plant Biol.* 2010;52(6):528–35.
- Skirycz A, Jozefczuk S, Stobiecki M, Muth D, Zanol MI, Witt I, et al. Transcription factor AtDOF4;2 affects phenylpropanoid metabolism in *Arabidopsis thaliana*. *New Phytol.* 2007;175(3):425–38.
- Rueda-Lopez M, Crespiello R, Canovas FM, Avila C. Differential regulation of two glutamine synthetase genes by a single Dof transcription factor. *Plant J.* 2008;56(1):73–85.
- Santopolo S, Boccaccini A, Lorrai R, Ruta V, Capauto D, Minutello E, et al. DOF affecting germination 2 is a positive regulator of light-mediated seed germination and is repressed by DOF affecting germination 1. *BMC Plant Biol.* 2015;15:72.
- Sugiyama T, Ishida T, Tabei N, Shigyo M, Konishi M, Yoneyama T, et al. Involvement of PpDof1 transcriptional repressor in the nutrient condition-dependent growth control of protonemal filaments in *Physcomitrella patens*. *J Exp Bot.* 2012;63(8):3185–97.
- Feng BH, Han YC, Xiao YY, Kuang JF, Fan ZQ, Chen JY, et al. The banana fruit Dof transcription factor MaDof23 acts as a repressor and interacts with MaERF9 in regulating ripening-related genes. *J Exp Bot.* 2016;67(8):2263–75.
- Jiao K, Li X, Su S, Guo W, Guo Y, Guan Y, et al. Genetic control of compound leaf development in the mungbean (*Vigna radiata* L.). *Hortic Res.* 2019;6:23.
- Hill JT, Demarest BL, Bisgrove BW, Gorski B, Su YC, Yost HJ. MMAPPR: mutation mapping analysis pipeline for pooled RNA-seq. *Genome Res.* 2013;23(4):687–97.
- Kang YJ, Kim SK, Kim MY, Lestari P, Kim KH, Ha BK, et al. Genome sequence of mungbean and insights into evolution within *Vigna* species. *Nat Commun.* 2014;5:5443.
- Jiao K, Li X, Guo W, Yuan X, Cui X, Chen X. Genome re-sequencing of two accessions and fine mapping the locus of lobed leaflet margins in mungbean. *Mol Breeding.* 2016;36(9):128.
- Su S, Xiao W, Guo W, Yao X, Xiao J, Ye Z, et al. The CYCLOIDEA-RADIALIS module regulates petal shape and pigmentation, leading to bilateral corolla symmetry in *Torenia fournieri* (Linderniaceae). *New Phytol.* 2017;215(4): 1582–93.
- Tamura K, Stecher G, Peterson D, Filipiński A, Kumar S. MEGA6: molecular evolutionary genetics analysis version 6.0. *Mol Biol Evol.* 2013;30(12):2725–9.
- Zhai C, Zhang Y, Yao N, Lin F, Liu Z, Dong Z, et al. Function and interaction of the coupled genes responsible for Pik-h encoded rice blast resistance. *PLoS One.* 2014;9(6):e98067.

49. Yoo SD, Cho YH, Sheen J. Arabidopsis mesophyll protoplasts: a versatile cell system for transient gene expression analysis. *Nat Protoc.* 2007;2(7):1565–72.
50. Sairam RK, Dharmar K, Chinnusamy V, Meena RC. Waterlogging-induced increase in sugar mobilization, fermentation, and related gene expression in the roots of mung bean (*Vigna radiata*). *J Plant Physiol.* 2009;166(6):602–16.
51. Su S, Shao X, Zhu C, Xu J, Lu H, Tang Y, et al. Transcriptome-wide analysis reveals the origin of *Peloria* in Chinese cymbidium (*Cymbidium sinense*). *Plant Cell Physiol.* 2018;59(10):2064–74.
52. Coen ES, Romero JM, Doyle S, Elliott R, Murphy G, Carpenter R. *Floricaula*: a homeotic gene required for flower development in *antirrhinum majus*. *Cell.* 1990;63(6):1311–22.
53. Qi H, Xia FN, Xie LJ, Yu LJ, Chen QF, Zhuang XH, et al. TRAF family proteins regulate autophagy dynamics by modulating autophagy protein stability in *Arabidopsis*. *Plant Cell.* 2017;29(4):890–911.
54. Clough SJ, Bent AF. Floral dip: a simplified method for agrobacterium-mediated transformation of *Arabidopsis thaliana*. *Plant J.* 1998;16(6):735–43.
55. Konishi M, Sugiyama M. A novel plant-specific family gene, root primordium defective 1, is required for the maintenance of active cell proliferation. *Plant Physiol.* 2006;140(2):591–602.

Publisher's Note

Springer Nature remains neutral with regard to jurisdictional claims in published maps and institutional affiliations.

Ready to submit your research? Choose BMC and benefit from:

- fast, convenient online submission
- thorough peer review by experienced researchers in your field
- rapid publication on acceptance
- support for research data, including large and complex data types
- gold Open Access which fosters wider collaboration and increased citations
- maximum visibility for your research: over 100M website views per year

At BMC, research is always in progress.

Learn more biomedcentral.com/submissions

